WP2 D2.2: Comparison Between HiL in Wind & Wave Tests

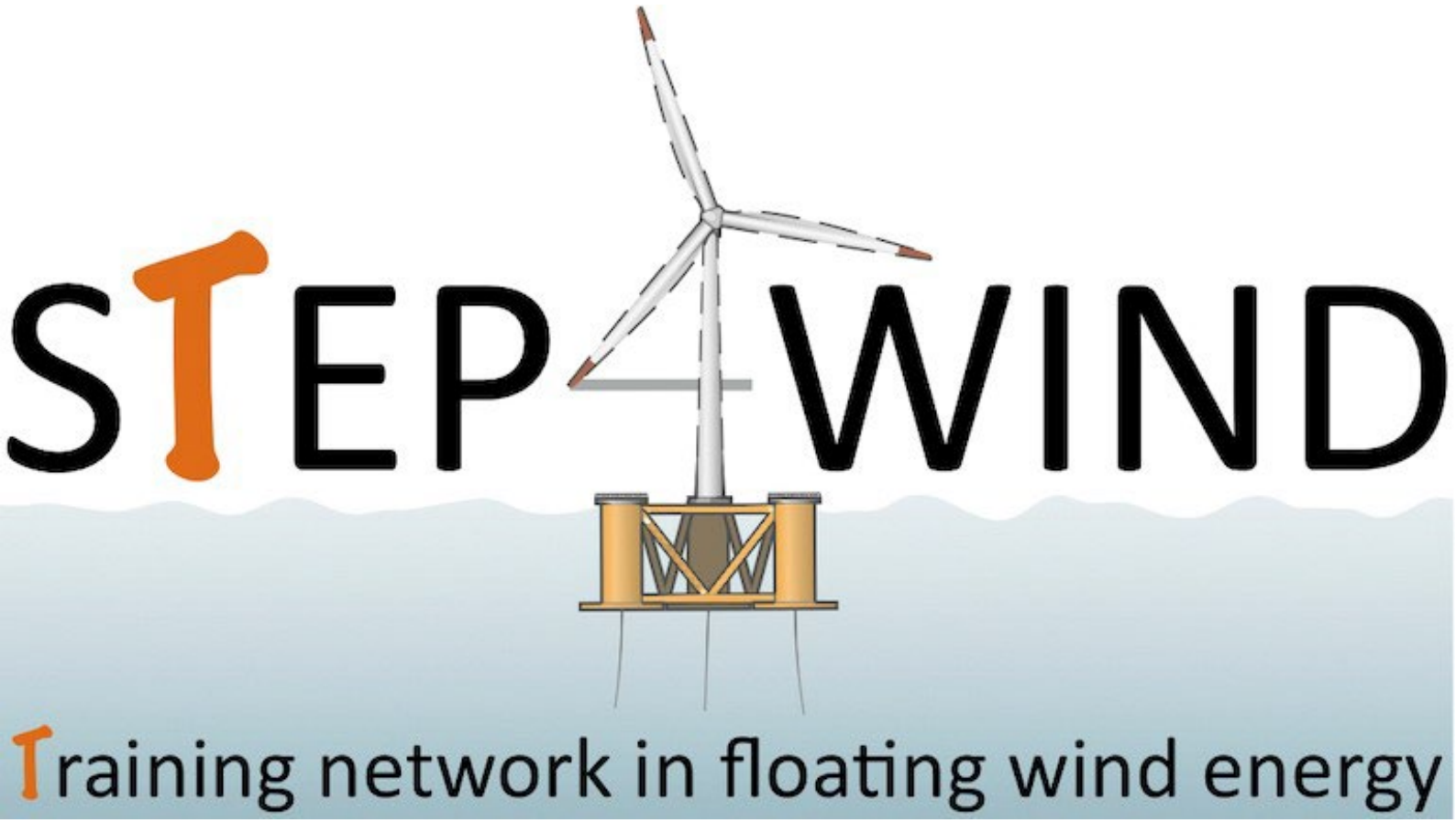

This project has received funding from the European Union's Horizon 2020 research and innovation programme under grant agreement No. 860737.

Document History

Revision Nr	Description	Author	Review	Date
V0.1	Comparison Between HiL in Wind & Wave Tests	Felipe Miranda Novais Industrial supervision: MARIN Academic supervision: Polimi	Oana Trifan (TU Delft)	28.03.2024

Index

1. Introduction 4
2. Wind Tunnel Testing 5
3. Wave Basin Testing 5
4. Experimental Setups 7
4.1. Wind Tunnel Setup 7
4.2. Wave Basin Setup 8
5. Numerical Comparison 11
1.1.1. Winch System 13
1.1.2. Wind Tunnel 14
1.1.3. Wind Tunnel 15
1.1.4. Wave Basin 17
6. Conclusion 20
7. Bibliography 22

1. Introduction

Up to date, the prevailing method of installing offshore wind turbines is to mount them on top of support structures rigidly affixed to the seabed. Nevertheless, these fixed foundations are economically viable only in water depths of approximately 60 meters or less (van Kuik et al., 2016). A way to overcome the sea depth limitations imposed by the financial cost of the traditional bottom-fixed structures is to place the wind turbines on top of a floating structure anchored to the seabed, expanding the utilization of the technology to harness the wind in deeper water, where is estimated to be 80% of the potential resources (GWEC, 2022).

The technological feasibility of Floating Offshore Wind Turbines (FOWTs) has already been attested in several pilot projects, examples range from cases such as the Hywind demo unit, where only a 2MW single turbine was first tested, to multi-megawatt wind farms, as the Kincardine, containing a 2 MW and five 9.5 MW windmills. With costs expected to decrease as the technology matures, it is predicted that floating wind will reach 2 % of the world's supply of energy by 2050 (DNV-GL, 2020). Nevertheless, currently, there are still many technical challenges to overcome in order to further push the employment of the technology and reduce its levelized cost of energy (LCOE).

Modern wind turbines can reach hub heights up to 150 meters, using as a reference the IEA-15 MW (Gaertner et al., 2020), and the tendency is for these machines to grow larger and larger. Installing a massive windmill on a floater structure that is subject to motions over the six-degrees-of-freedom is a complex task, especially when it comes to the structural dynamics and aerodynamic interactions entailed in these systems. Due to the intricate dynamics presented in FOWTs, it becomes essential to thoroughly comprehend the loads experienced during operation and assess the reliability of existing numerical models utilized in the design process.

A common practice utilized by both the maritime industry for research and development of floating structures is to make use of scale models, an approach that allows, under a controlled environment, to investigate the behavior of the whole system at a lower cost and shorter time span when compared to full-scale prototyping. Model test of FOWTs has been a valuable tool at this early stage of the industry as means to understand the overall dynamics of the system, identify the presence of any unforeseen phenomena, evaluate the system’s response under extreme environmental conditions as well as provide a benchmark for validating numerical models (DNV-GL, 2019). Indeed, code comparison campaigns, such as the OC5 Phase II (Robertson et al., 2017), made a significant effort to compare different engineering tools utilized by both the industry and the academia, noticing an underprediction of ultimate and fatigue loads by several medium-fidelity simulation codes when compared to physical experiment, reinforcing the importance of model testing to mitigate risks and uncertainty involved on the development of the technology.

Nowadays, different techniques for performing experiments with FOWT are available, each with its strengths and limitations. Reproducing accurately the aerodynamics and hydrodynamics in an experimental facility is a challenging task and each approach might be more suitable for a specific goal or even used in conjunction to bypass experimental limitations and exploit the advantages of each method in a synergetic way. This paper aims to present a comparison between wave basin and wind tunnel techniques, focusing more specifically on the setups developed by the Maritime Research Institute Netherlands (MARIN) and the Politecnico di Milano. The experimental setups were based on the same platform, the goal is to present a numerical analysis by comparing the gathered data against numerical models and that way, elaborate on the potential weaknesses and strengths of the different experimental setups investigated.

2. Wind Tunnel Testing

Wind tunnel facilities, with their capacity to produce a high-quality and well-controlled wind field, serve as an ideal location for conducting experimental assessments of wind turbine aerodynamics. Given the absence of waves, a mechanical apparatus is required to induce movements and replicate the motion at the tower base of the scaled model. This kind of approach is particularly useful to understand the changes in the aerodynamic loads and wake development of floating offshore wind turbines when subject to wave motion.

An application of wind tunnel testing is gaining insight into the unsteady aerodynamics present in FOWTs. In Bayati et al. (2016c) the author performed a comparison between a Blade Element Momentum (BEM) code and experimental data when the turbine is subject to both pitch and surge motions, the results were inconclusive, which was later attributed to the tower's flexibility. The outcome of that study motivated a new test campaign, the UNAFLOW project (Fontanella et al., 2021), focusing solely on surge motion and performing tests covering an ample range of amplitudes and frequencies to delve into the effects that the motion has over the measured thrust, torque and wakes, which were measured using a particle image velocimetry (PIV) and a hot-wire measurements. Similarly, cooperative actions, namely the OC6 Phase III (Bergua et al. 2023), utilized the wind tunnel data from the same rotor, to perform a cross-comparison between codes of different degrees of fidelity for both surge and pitch. In Taruffi et al. (2024), the experimental measurements from harmonic prescribed motions were compared to quasi-steady prediction for surge, pitch and yaw, going beyond the reduced frequencies previously tested and observing unsteady behavior at high-frequency motions.

In addition to employing open-loop-based approaches, in which the actuator is set to perform a prescribed motion, usually sinusoidal, over the degrees of freedom of interest, it is also possible to apply a closed-loop approach, where physical measurements are connected to the control system of the actuator's motion. A hybrid Hardware-In-the-Loop (HiL) method was developed by Politecnico di Milano, where the aerodynamic forces are measured physically and fed to a simulation environment that calculates the hydrodynamic forces. The coupling is possible due to a 6-component force transducer placed at the connection point between the tower's base and the robotic actuator device. The measured forces are corrected, to eliminate inertial contribution and account for only the purely aerodynamic forces that the physical rotor is subject to and sent to a numeral model that accounts for the hydrodynamics and wave loads, performing then, real-time integration of the platform coupled rigid-body motion. This methodology was first applied in Bayati et al. (2020), where a two Degree-of-Freedom (DoF) hydraulic actuator was used to emulate the pitch and surge dynamics of the platform, but in follow-up studies, the setup was substituted by a 6 DoF, parallel kinematic robot, named Hexafloat, which was already utilized in to investigate the coupled dynamics of a OO-Star floater and a DTU 10 MW turbine (Belloli et al., 2020).

3. Wave Basin Testing

In order to replicate, in a wave basin, the floater and wave dynamics of the full-scale prototype it is necessary to apply the Froude scaling. Nevertheless, the dissimilitude between the Reynolds and Froude scaling laws represents a challenge when it comes to testing FOWTs. Given the strong coupling between aerodynamics and hydrodynamics involved in these systems, it is crucial to accurately reproduce the physics involved in the rotor as well as the floater and mooring lines. Therefore, by simply applying

Froude scaling to the system of interest, there will be a compromise in the model's ability to represent with fidelity the overall dynamics of a real turbine in the open sea.

In Goupee et al. (2012) three floater concepts, with a scale factor of 1:50, were tested using the reference NREL 5 MW turbine (Jonkman et al., 2009) at the MARIN. However, for that test campaign, Froude-scaling was applied to the whole system. Consequently, what was noticed was an underperformance of the rotor, presenting a thrust that was significantly lower than expected in addition to negative torque when the turbine was under operating conditions.

For the accurate representation of a FOWT, it is ideal to reproduce thrust and torque values at model scale. Given that the aerodynamic torque is not as relevant for the system dynamics as the overturning moment generated due to the thrust under operating conditions, adaptations are needed mainly to ensure a correct thrust. One workaround is to increase the generated wind speed until the thrust force reaches its desirable value, yet, by doing so the tip-speed ratio is not maintained, which is not ideal since it impacts the aerodynamic torque and the rotor passing frequencies (Müller et al., 2014). Another solution for dealing with the challenges set by the Froude-scaled wind is to design the blade utilizing a specific airfoil profile that is suitable for a low-Reynolds environment, a process referred to as performance scaling (Martin et al., 2014) (Fowler et al., 2013).

Following the initial test campaign in Goupee et al. (2012), a new performance scale rotor properly adjusted to match the thrust of the reference turbine was utilized in Goupee et al. (2014) with the same three floating platforms concepts. The setup, using specifically the semi-submersible floater, was later utilized as the reference for the code-to-experiment comparison performed during the OC5 Phase II (Robertson et al., 2017) and one of the observations was the difference of agreements depending on the modeling approach employed, underscoring the significance of model testing as a means to evaluate the robustness of numerical tools.

Even though utilizing an experimental wave basin setup with a physical turbine, considering that the blades are properly adjusted to meet the target thrust, allows for the investigation of the fully-coupled dynamics with also the possibility of revealing phenomena that are not yet known and characterized by numerical models, there are many challenges when it comes to generating a wind field inside this kind of facility. In a wave basin, the re-circulation of the flow and the control of the wind field are among the main bottlenecks (Gueydon et al., 2020), furthermore, the infrastructure needed, such as a bigger basin and system of wind fans, also represents an additional financial cost.

In a wave basin, the hybrid approach consists of substituting the rotor-nacelle assembly by an actuator system. The concept is to utilize a device that is capable of emulating the aerodynamic loads and the rotor's response coupled to the floater motions, that is, the platform displacement and velocities are measured by a set of sensors and are fed to a numerical model that is calculating the forces to be imposed by the actuator. One of the main advantages of this approach is that it allows to numerically set the wind field and aerodynamic forces, and hence, eliminate the undesired effects of the Froude-Reynolds scaling and the constraint of physically generating a wind field. Up to date, this methodology has been used with different kinds of devices, such as ducting fans, citation, drone propellers, citation, and cable-driven robots (Gueydon et al., 2020).

The utilization of a hybrid approach also presents limitations, which are mainly dictated by the capabilities of the utilized actuator system and the numerical models utilized. In Hall et al. (2014), the performance requirements for the choice of actuator device are discussed. Due to the necessity of having the aerodynamics simulated in real-time, there is a requirement for some degree of simplification of the running numerical model to decrease the computational cost. In Bachynski et al. (2015), an examination was carried out to assess how simplifying certain aspects of aerodynamic physics would impact the motion of the platform. In certain situations, it's worth noting that the actuator may not be able to replicate motion across all six degrees of freedom. For instance,

when utilizing a ducted fan, the aerodynamic forces are restricted solely to the thrust force, when using a winches, the space constraint might also limit the amount of reproducible axis of motion. Among the advantages of utilizing a cable winch system as an actuator is that it presents low-vibration levels and less systematic uncertainty (Otter et al., 2022).

4. Experimental Setups

The setups utilized in this paper are from two facilities. A wind tunnel hybrid setup from Politecnico di Milano and two different wave basin setups from MARIN, one featuring a physical wind turbine and the other equipped with a winch actuator, both utilizing the same scaling factors. Table 1 presents the scaling factors of the models utilized.

Table 1. Scaling factors for the wave basin and wind tunnel models utilized.

Scale Factor	Wind Tunnel Model Expression	Wind Tunnel Model	Wave Basin Models Expression	Wave Basin Models
Length (λ_L)	-	53	-	50
Velocity (λ_V)	-	3	$\lambda_L^{1/2}$	7.07
Time (λ_t)	λ_L/λ_V	17.67	$\lambda_L^{1/2}$	7.07
Frequency (λ_f)	λ_V/λ_L	0.06	$\lambda_L^{-1/2}$	0.14
Acceleration (λ_n)	λ_L^3	0.17	λ_L^0	1
Mass (λ_M)	λ_L^3	148877	λ_L^3	125000
Force (λ_F)	$\lambda_L^2 \cdot \lambda_V^2$	25281	λ_L^3	125000
Torque (λ_T)	$\lambda_L^3 \cdot \lambda_V^2$	1339893	λ_L^4	6250000
Reynolds (λ_R)	$\lambda_L \cdot \lambda_V$	159	$\lambda_L^{3/2}$	353.55

4.1. Wind Tunnel Setup

The wind tunnel data utilized in this paper is extracted from the test campaign performed in Bayati et al. (2020). The 1:75 model of the DTU 10 MW (Bak et al., 2013) was mounted on the 2-degrees-of-freedom test rig, Figure 1. The platform utilized during the experiment is the DeepCWind semi-submersible scale model, the floater numerical model was calibrated to match the experimental data performed during the OC5 Phase II test campaign. Since the DTU 10 MW was designed based on a direct upscale of the NREL 5 MW, the scaling factor was adjusted in an order of √2, representing approximately a 1:53 scale model of the NREL 5 MW. The rotor was designed to operate at the low-Reynolds conditions that are found in wind tunnel testing, the scaling process is presented in Bayati et al. (2016).

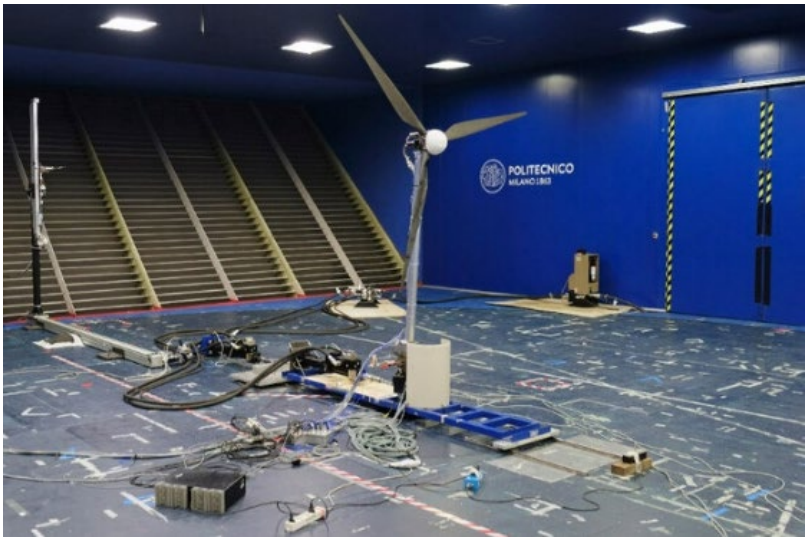

Figure 1.HiL wind tunnel model

4.2. Wave Basin Setup

The results presented in this paper are relative to two wave basin setups. The first utilizes the full physical rotor with the Marin Stock Wind Turbine (MSWT) and the second utilizes a winch frame actuator system, the setups are shown in Figure 2. The platform and mooring lines are kept the same. A schematic drawing of the two models is presented in Figure 3, the hub height of the MSWT, is located at the same place where the main winches are connected. The winch frame was projected to mimic the mass characteristics of the MSWT, a Table 2 shows exactly the upscaled inertial properties of each system compared.

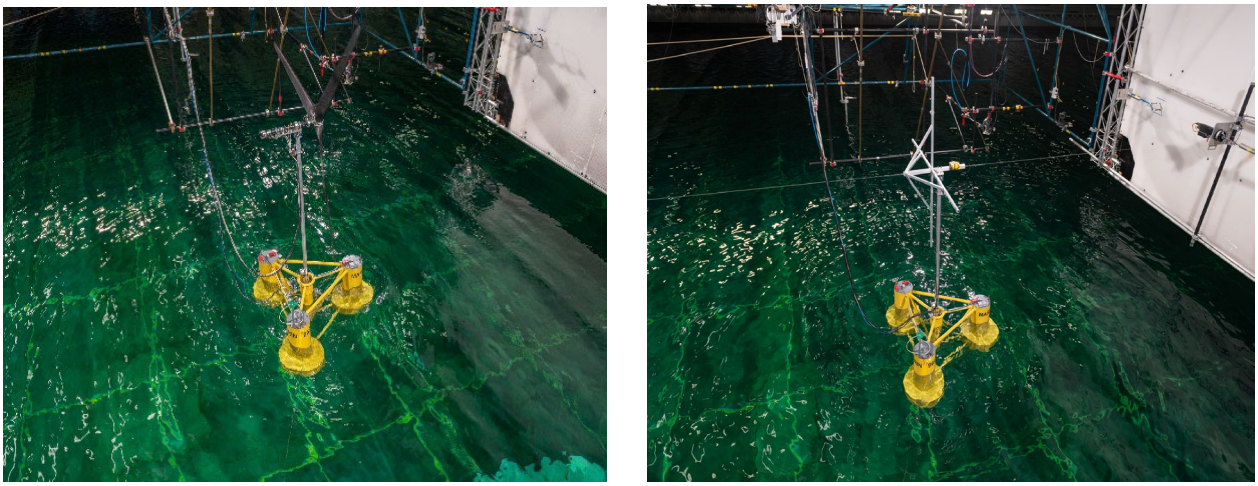

Figure 2. Setup with a physical rotor (left), and with a winch frame (right).

Table 2. Full scale inertial properties of both wave basin setups.

System A	MSWT	Winch
Mass [ton]	662.85	658.4
Gx [m]	0.12	0.12
Gy [m]	0.0	0.0
Gz [m]	-0.12	-0.37
Kxx [m]	16.09	9.23
Kyy [m]	14.6	11.82
Kzz [m]	14.6	11.82

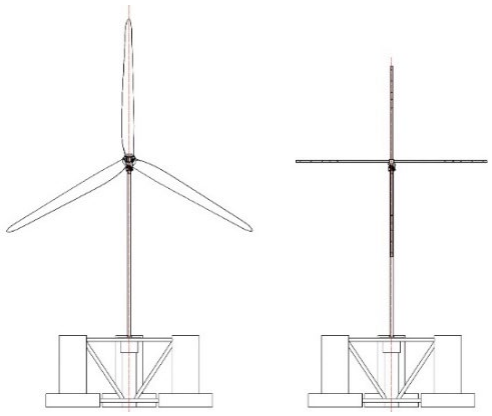

Figure 3. Drawing of the floater with the MSWT (left) and with the winch system (right).

The schematics of the software-in-the-loop system is seen in Figure 4. Two pulling cables are connected to the central point of the frame, located at the aft and fore-aft positions. The front winch is responsible for compensating for pretension applied by the rear winch. The software-in-the-loop works by determining the forces and moments based on the position, velocity and the wind time-series that are fed to the algorithm, which in this case, is a BEM model using the Aerodyn v13 interface with a basic BEM model implementation considering the rotor fully rigid, without any dynamic stall model, no tower influence is considered and applying Prandt model tip and hub -losses. The forces and moments that are calculated are applied according to Froude law. It is also important to highlight that the setup utilized in this project is capable of only applying Fx forces. Therefore, the full dynamics of the system over the 6-DoF is not fully captured; however, the most important force component, the thrust, is represented by the Fx forces.

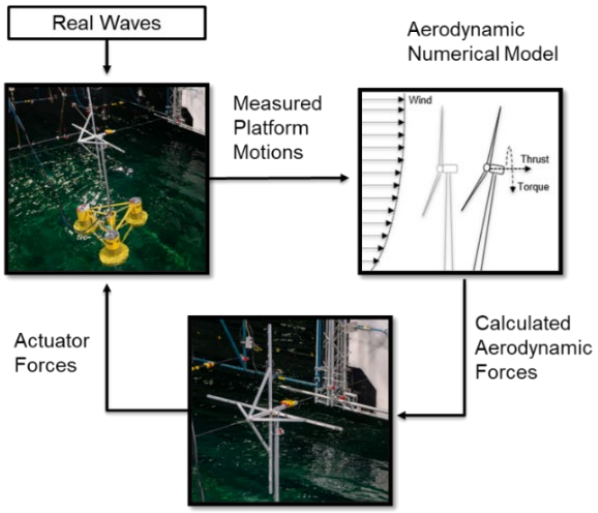

Figure 4. Schematic of the wave basin hybrid approach.

The generation of physical wind at the wave basin is possible due to a wind outlet that consists of 42 fans rotating at a fixed or varying rpm, capable of generating steady and turbulent wind, Figure 5. Two honeycombs are utilized to avoid swirls and straighten the flow, and thus, generate a more uniform and steady wind across the section. The quality of the wind field can be visualized in Figure 6, where it can be seen that the points around the centre of the nozzle present lower turbulence, around 5, whereas it is observed up to 25% near the edges. The rotor of the MSWT, due to its smaller size when compared to the outlet nozzle, is not heavily influenced by the differences observed near the edges.

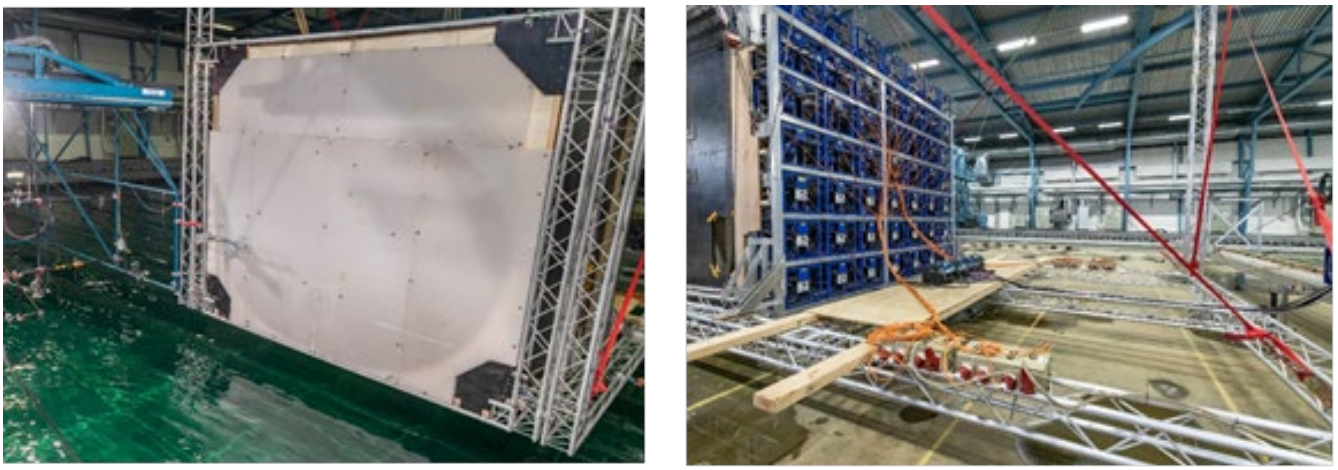

Figure 5. Front-view (left) and Aft-view (right) of the wind nozzle.

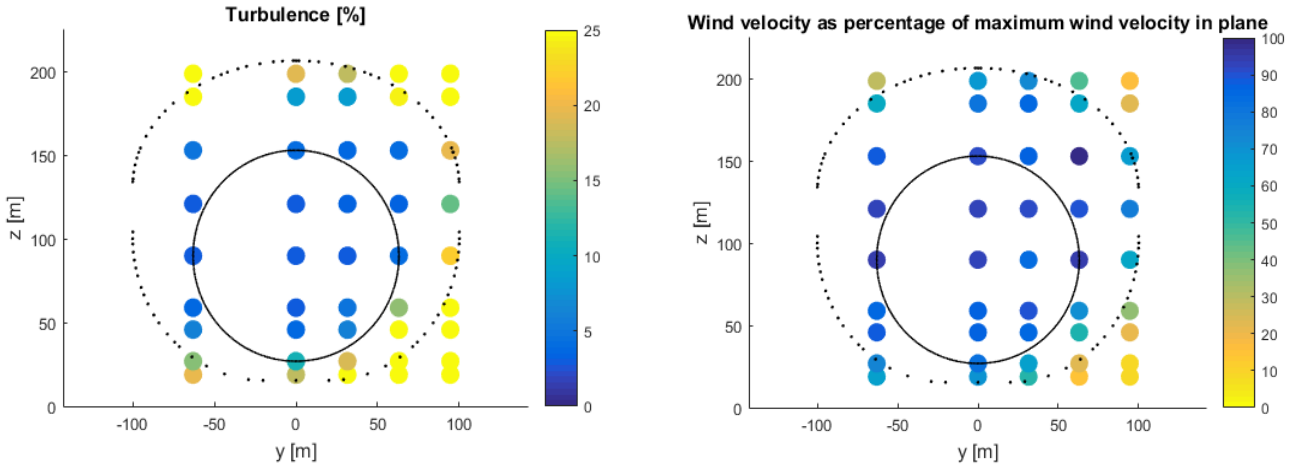

Figure 6. Wind field turbulence as a percentage of maximum wind velocity in the plane (left) and wind field velocity as percentage of maximum wind velocity in plane (right). The dashed black elliptical mark represents the wind nozzle outlet size and the solid black circular line is the rotor area.

5. Numerical Comparison

Given that there is a mismatch between wind and wave conditions utilized between the basin and the wind tunnel tests, it is not possible to make a direct comparison. Therefore, the main idea of this study is to investigate what differences are observable between the typically used medium-fidelity numerical codes and the gathered experimental data.

Two numerical models based on FAST v8 (Jonkman and Jonkman, 2016) were utilized:

- FAST Wave Basin: The FAST model utilized for the comparison with the wave basin experimental data is based on the model developed during the OC5 Phase II project. A calibration of the numerical model was performed in order to ensure that the hydrodynamic loads and rigid-body dynamics were consistent with the experiments. More information regarding the elaboration and validation of the OC5 FAST model can be found in Wendt et al. (2019).
- FAST Wind Tunnel: Given that the wind turbine rotor utilized at the wind tunnel was different from the one utilized during the OC5 project, the model needed to be adjusted to better represent the experiments. The polar and distributed blade properties utilized were changed to match the ones of the real wind tunnel model. The floater model utilized is the same that is the DeepCWind Semisubmersible.

The test matrix is presented in Table 3. For the wave basin tests, both setups were tested under the conditions presented and a broad-spectrum signal, called ramped noise was utilized to investigate the response of the system for different frequencies. The wind tunnel conditions were selected based on the main results that were published in Robertson et al. (2017) and are wave conditions that were also tested during the OC5 Phase II.

Table 3. Test matrix.

	Test	Vw [m/s]	Hs [m]	Tp [s]	γ [-]	β [deg]	ω [rpm]
Wave Basin	Wave Only	0	10.5	6 - 26	-	90	-
	Near Rated	13				6	12.1
	Above Rated	21				17.2	12.1
Wind Tunnel	Wave Only	0	7.1	12.1	2.2	90	-
	Below Rated	9				-3.5	10.2
	Rated	11.4				-1	13.5
	Above Rated	14				7.2	13.5

Where *Vw* is the steady wind speed, *Hs* is the significant wave height, *Tp* is the wave peak-spectral period, γ is the wave peak-shape parameter, β is the blade pitch angle and ω is the rotor speed.

5.1. Decays

Free decay tests across the experimental setups and the numerical models to assess the natural frequencies and damping characteristics were performed and the results are shown in Table 4.

Table 4. Natural frequencies of the numerical models and experimental setups investigated.

Degree-of-Freedom	MSWT	Winch	FAST Wave Basin	WTM	FAST WTM
Surge [Hz]	0.0088	-	0.0090	0.0090	0.0090
Sway [Hz]	0.0086	-	0.0096	-	-
Heave [Hz]	0.0568	-	0.0576	-	-
Roll [Hz]	0.0313	-	0.0314	-	-
Pitch [Hz]	0.0314	0.0312	0.0292	0.032	0.031
Yaw [Hz]	0.0121	-	0.0121	-	-

5.2. Analysing the Effects of the Actuator Over the Motion

1.1.1. Winch System

To assess the impact that the winch has over the motion, two configurations were tested for the same wave condition with the winch system. Firstly, the winches were completely disconnected from the frame, and afterward, were reconnected and set to deliver zero loads. The “following mode” involves calibrating the winch to equalize tension in response to the motion induced by the waves and it is a way to investigate if the tension of the cables is lagging or impairing the system’s response at any given frequency. This methodology for accessing the influence of the winch over the motion was first presented in Gueydon et al. (2016). To conduct the analysis, it is necessary to make sure that the wave conditions are aligned between both tests. Figure 7 shows the Power Spectra Density (PSD) of the wave in both scenarios, the wave conditions were quite comparable, with the disconnected lines cases showing a slightly higher energetic spectrum.

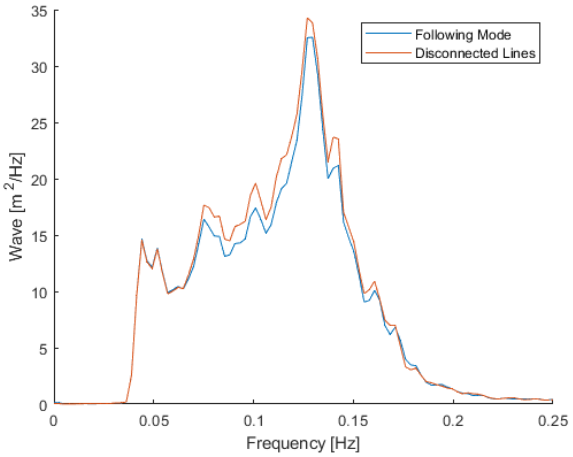

Figure 7. PSD of the wave conditions for both tests.

In Figure 8, the results of the Response Amplitude Operators (RAOs) for pitch and surge are shown. Concerning the pitch motion, it can be seen that the cables are leading to minor damping mainly at the pitch natural frequency, it is also observed that for higher frequencies, at around 0.17 Hz, there was a difference in phasing between both configurations, indicating that beyond that range, the winch will lag in delivering the requested forces in real-time. Nevertheless, given that most of the wave spectrum energy is located below 0.175 Hz, the effect of the lag at such frequency shouldn’t cause any major impact. For the surge, the winch tension is affecting the natural frequency of the setup and also damping at the surge natural frequency. In summary, it can be concluded that the winch influences primarily the motion on the system’s natural frequency, damping the response of the turbine, and also lag in delivering the requested forces at higher frequencies.

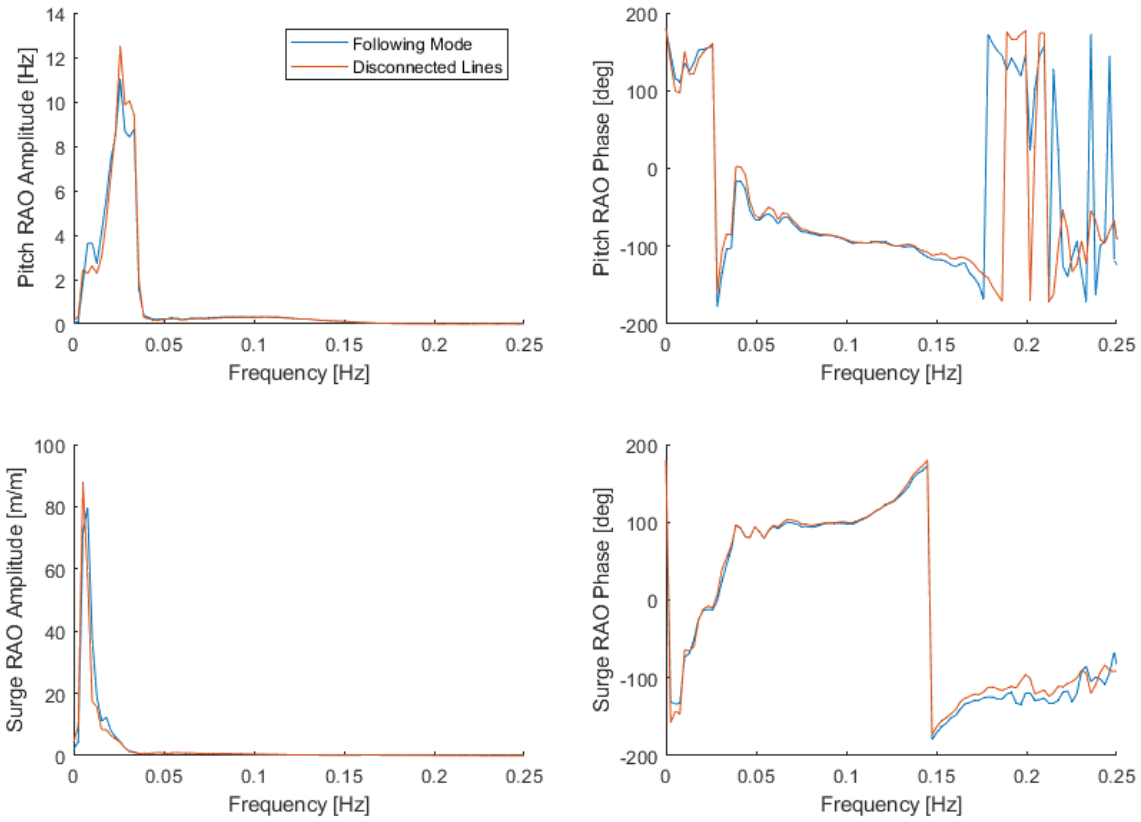

Figure 8. RAOs of the pitch and surge motion for the platform with the winch on following mode and the winches disconnected.

1.1.2. Wind Tunnel

To evaluate the hexapod's ability to replicate the desired motion, a test involving only waves was carried out. The idea consists of comparing the HiL setpoint that is internally calculated by the numerical model with the actual motions that were measured by an external sensor, a linear velocity displacement transducer (LVDT).

The PSD of the wave elevation spectra, utilized is shown in Figure 9 as well as the PSDs of the motion for pitch and surge, are presented in Figure 10. It can be seen that the pitch is damped especially in the wave frequency region. In summary, it is noted that the actuator primarily disrupts pitch motion within the wave frequency range, with minimal influence on lower frequencies and no discernible impact on surge motion.

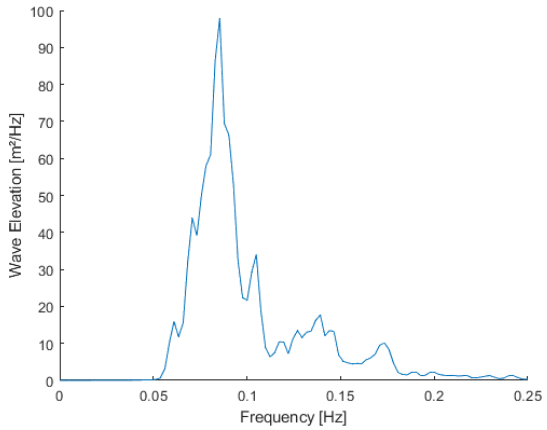

Figure 9. PSD of the wave elevation utilized for the test.

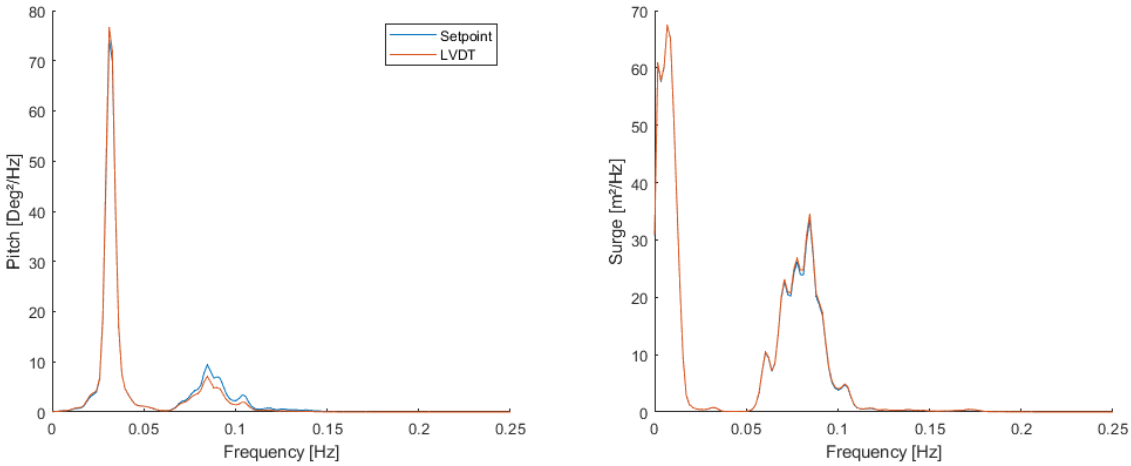

Figure 10. Comparison between the setpoint of the HiL and the measured motion by the LVDT sensor for the pitch (left) and surge motions (right).

5.3. Wind and Waves

1.1.3. Wind Tunnel

The power spectral density of pitch for the four wind conditions is depicted in Figure 11. Firstly, it is noticeable that the experimental data presented a different behavior on the peaks at the pitch natural frequency for the “No Wind” and “Below” wind cases. On the other hand, a closer match in response for the “Rated” and “Above” wind conditions is observed. At the wave frequency, the experimental cases indicated a greater level of damping that is caused by the actuator, as noted earlier. Nevertheless, what is observed is that overall, the experimental data presented a higher damping at the pitch natural frequency with respect to the condition without wind. Identifying the precise reasons for this disparity is challenging due to the complexity of the system and the lack of measurement repetition to assess the systematic uncertainty. Furthermore, the HiL numerical model implemented was not

investigated in-depth, which could be one of the explanations for the observed trend. Similar questions also arise when observing the surge response, Figure 12, where higher peaks are observed at the low-frequency region.

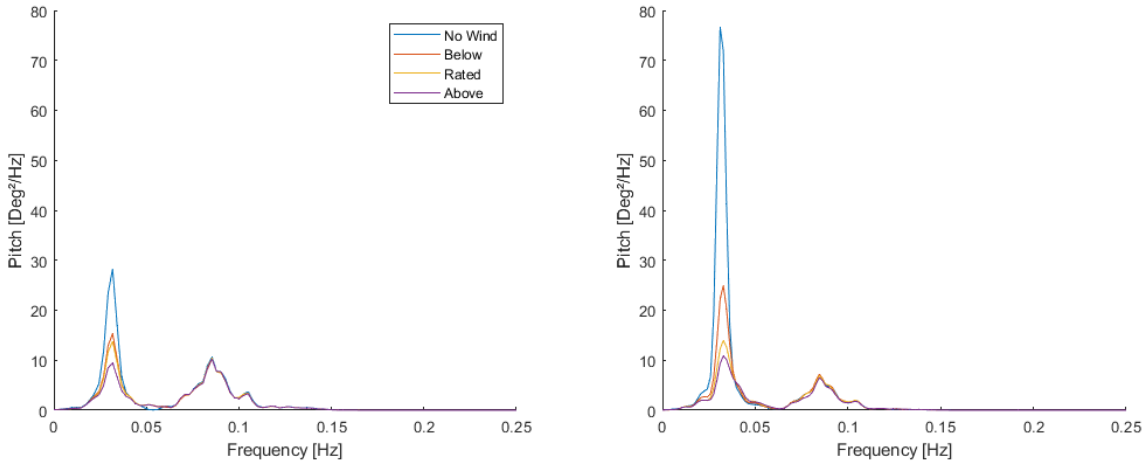

Figure 11.PSDs for the pitch motion of FAST (left) and the Experiment (right).

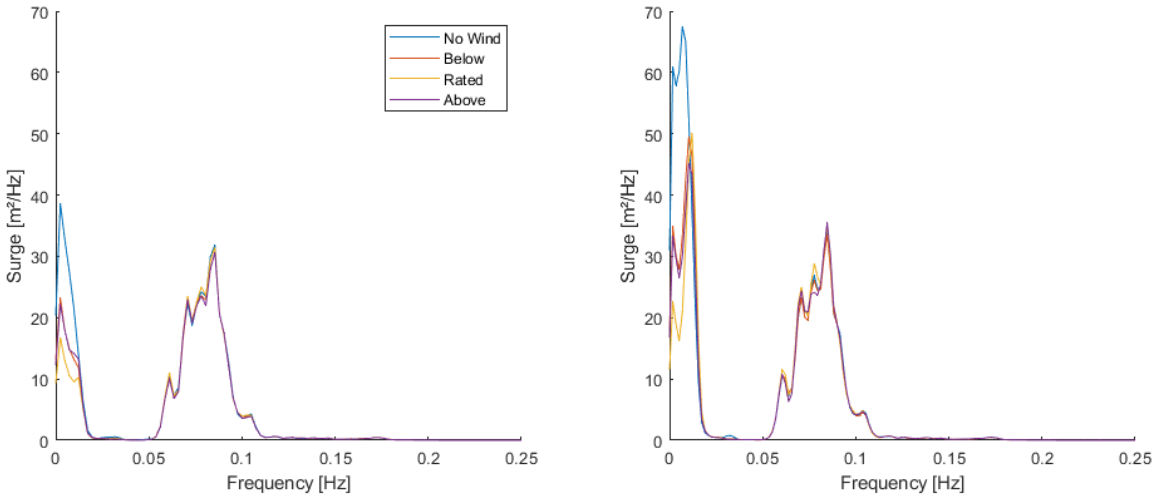

Figure 12. PSDs for the surge motion of FAST (left) and the Experiment (right).

During the test campaign, pitch decay tests with wind were also performed, the idea was to assess whether the damping observed for the HiL would be higher than in the numerical simulations. Figure 13 illustrates the results presented in Bayati et al. (2020), the damping as seen is slightly higher during the experiment. This could suggest that the experimental damping is marginally higher than that predicted by the numerical model utilized. Nevertheless, the actuator might be also introducing damping to the system's response, which was not quantified during this experiment.

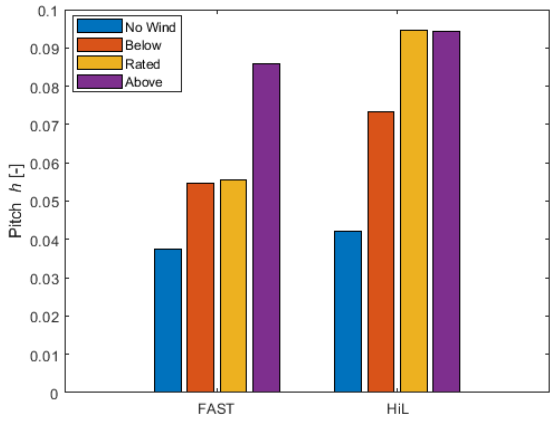

Figure 13. Platform damping (h) for the pitch decays tests with wind for the FAST numerical model and the HiL experiment.

A box and whiskers plot is shown in Figure 14, where good agreement between the experiment and numerical model can be seen, with the HiL presenting slightly lower medians for the pitch in the cases with wind, also with comparable inter-quantile ranges and flier values with slightly higher discrepancies observed for the “No Wind” case, as seen in Figure 11.

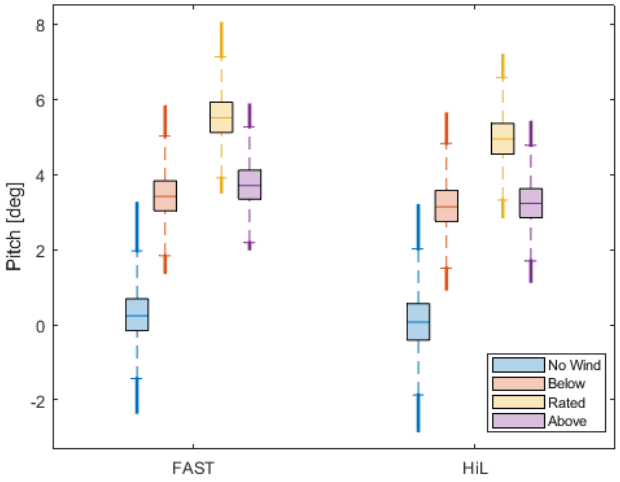

Figure 14. Box and whisker plot comparing the FAST simulations and the HiL experiment.

1.1.4. Wave Basin

The wave condition employed for the analysis is shown in Figure 15, clearly demonstrating the matching of conditions between the winch and MSWT. The FAST numerical model is provided with identical time-series data for wave elevation extracted from the experimental measurements, and similarly, the wind velocity time-series that is measured at the hub height is also utilized.

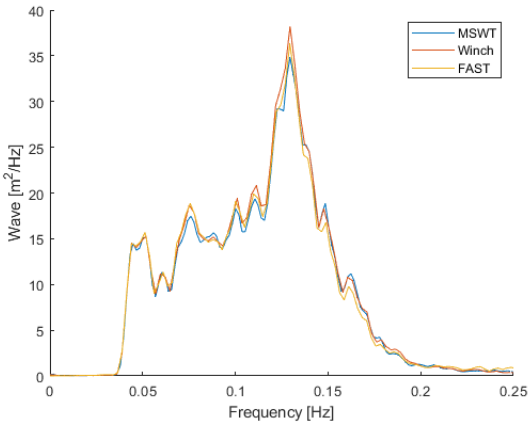

Figure 15. Power Spectra Density of the wave conditions for both tests.

For the 13 m/s case, Figure 16, it is observed that at wave frequency, the results are very consistent, with the main differences being evident in the low-frequency region for both pitch and surge between the experiment and the FAST model. Since there is no energy excitation from linear waves at these frequencies, the excitations must originate from non-linear forces. FAST's Hydrodyn models second-order potential flow excitation utilizing Quadratic Transfer Function (QTF) with Morison equation to model quadratic drag. The underprediction observed is very likely a consequence of higher-order wave hydrodynamic effects not captured by the numerical model utilized.

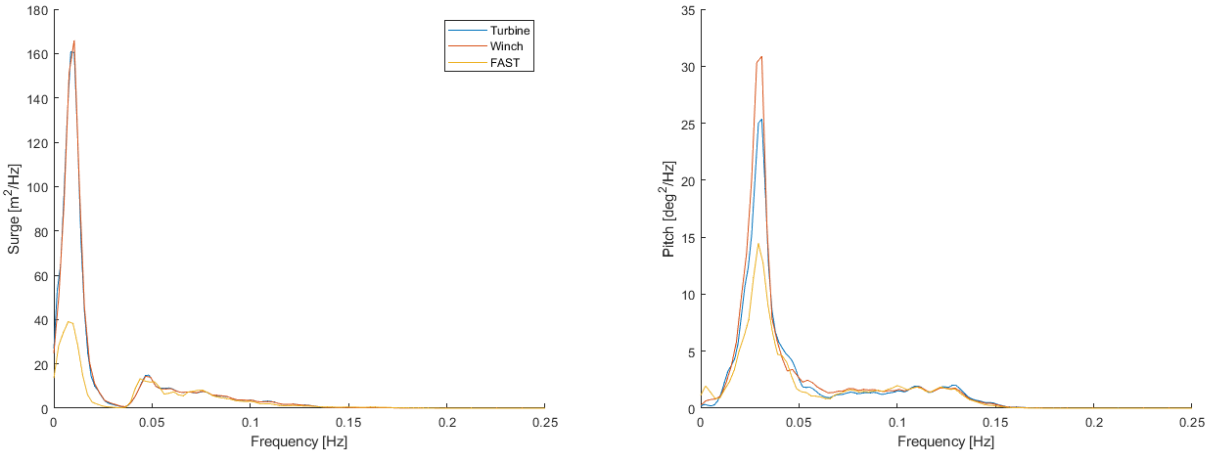

Figure 16. PSDs for the surge (left) and pitch (right) motions for the 13 m/s case.

Regarding disparities between the winch and the turbine, there are a few observations to highlight. Firstly, for the 13 m/s case, the winch added stiffness is causing a small deviation in the surge natural frequency, with a minor impact also on the motion amplitude. The most significant difference is noticed at the pitch peak, where there is a difference in the response between the

two systems. As mentioned in Gueydon et al. (2016), the aerodynamic damping acts mainly at the pitch natural frequency, and it could be suggested that the damping experienced by the turbine is higher than what is currently predicted by the BEM numerical model utilized. However, a conflicting result was observed for the 21 m/s case, Figure 17, where the turbine presented a lower peak when compared to the cable system. Overall, small deviations with respect to the pitch natural frequency were seen for the case with the physical turbine and FAST, considering the 13 m/s and 21 m/s cases, differently from the winch, which presented a significant variation.

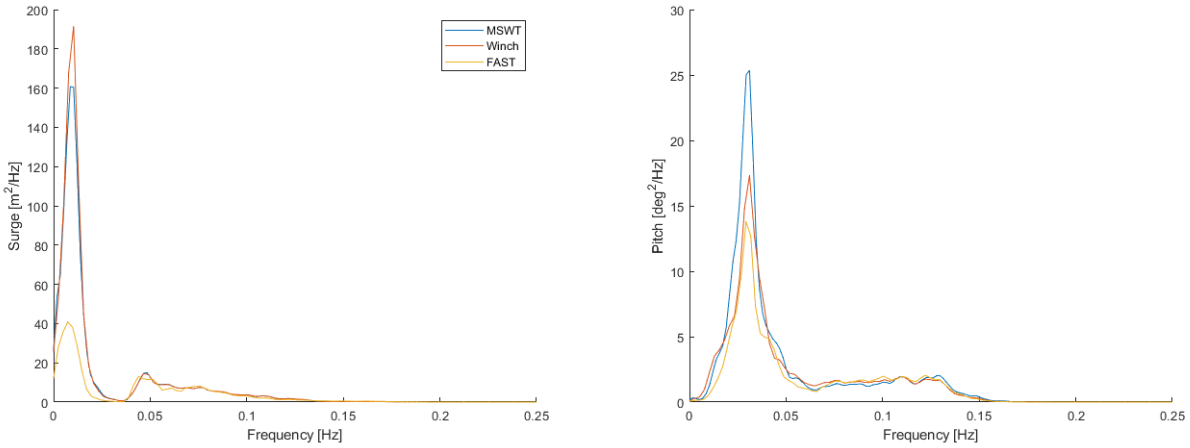

Figure 17. Power Spectra Density for the surge (left) and pitch (right) motions for the 21 m/s case.

Figure 18 shows a box-whisker plot for the wave basin results. The winch presented a higher pitch motion for the 13 m/s, where the thrust is higher, and a similar response for the case of 21 m/s. The FAST model underpredicts the median surge and presents a slightly lower pitch for the 21 m/s case.

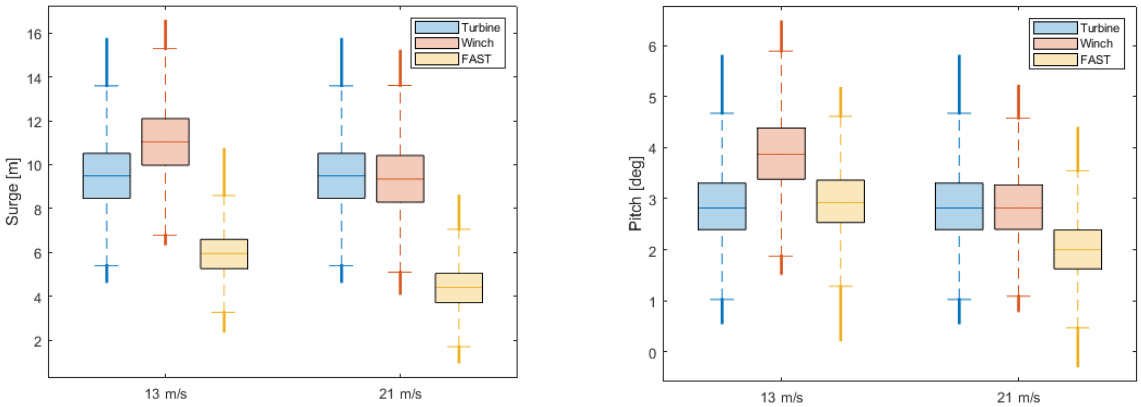

Figure 18. Box and whisker plot comparing the FAST simulations and the wave basin experiments.

6. Conclusion

Model testing of floating offshore wind turbines presents challenges given the intricate complex nature of the system being examined. Experimental methodologies were developed to better understand the physics involved, yet there are still limitations in its use. As highlighted in Gueydon et al. (2020), there remains a need for more critical comparison among emulation techniques and testing facilities to dimmish uncertainties. A valid approach to improve the comprehension of the coupled dynamics involved is to perform cross-validation, where different methodologies are used in combination and the strengths and limitations of each approach are put in perspective. This process enables researchers to validate their findings across multiple platforms, thereby enhancing the reliability and robustness of the results.

Previous work such as Thys et al. (2019) and LIFES50+ (2015), aimed at evaluating testing differences and providing guidelines for the combined use of HiL wind tunnel and wave basin testing. This work aimed to extend the discussion while also providing a quantitative analysis by comparing experimental results against the respective medium fidelity engineering tools commonly used for load analysis.

Concerning wind tunnel tests, the assumption is that the high quality and controlled wind field present at the facility is ideal for capturing all the aerodynamic phenomena involved when the turbine is under motion. An actuator is needed to provide the motion at the base of the tower and if the goal is to investigate real-time coupled dynamics, a HiL implementation is required, where a hydrodynamic numerical model is used in conjunction with the measured aerodynamic forces. The main challenges of using that approach are relying on the actuator, which needs to be capable of reproducing the very fast rotational motions involved, the simplifications in the hydrodynamic model to run in real-time and the complex inertia correction to extract just the aerodynamic component of the measured forces.

During the analysis, one of the observations was that at wave frequencies, the hexapod was not capable of replicating the demanded motion. Considering the reduced scale and for the specific platform studied, pitch motions at the wave frequency will require very high motion speeds and accelerations. Given that the size of the model is constrained by the size of the wind tunnel, in order to avoid blockage, the smaller the model, the higher and more challenging it will be to replicate such conditions, which might be a limiting factor of using this approach in facilities with small dimensions. Another point to consider is the simplifications that are needed for the HiL model to run in real-time, previous work such as Bayati et al. (2018) elaborates on some adaptations required. Nevertheless, by simplifying the running hydrodynamic model, a relevant part of the coupled dynamics is neglected, especially given that the medium-fidelity hydrodynamic models are not capable of fully capturing the semi-submersible low-frequency motion spectrum, as seen in the wave basin results.

The main observable difference between the results with wind and wave for the HiL test is the response at the pitch natural frequency. It is not clear if these differences were caused by the numerical implementation used in the HiL during the experiment or simply hardware shortcomings. Nevertheless, what could be noticed is that the HiL experienced a higher damping from the cases with no wind to the cases with wind. More investigation in this direction could reveal if indeed the damping in wind tunnel testing, as seen during the decays with wind presented, is higher than the typical BEM models. Also important to highlight that besides the HiL applications in a wind tunnel, the open-loop approach, which consists of predefining the motion, is still the golden experimental standard for the validation of aerodynamic models and investigation of the wake dynamics.

In relation to the wave basin tests, complex hydrodynamic interactions are physically present that are yet not well captured by the numerical models. As seen in the results, for that specific platform, there is still an underprediction of the numerical models at the low-frequency motion. When it comes to fully understanding the coupled dynamics, the wave-basin with a turbine model is still the preferred method given that by having both the hydrodynamics and the aerodynamics physically present it is possible to

capture phenomena that is not predicted by the current numerical tools. Despite the wind field being not ideal at a wave basin, depending on the size of the wind outlet nozzle and the rotor to be tested, the quality of the wind field might not be that compromised, as seen by the wind field measurements where near the edges, turbulence might reach up to 25%, whereas near the rotor, values only at about 5% when trying to emulate a steady wind condition. At a wind tunnel, using as reference the boundary layer section of the GVPM, the turbulence is only about 2%.

A wave basin hybrid approach is an alternative to deal with the high costs and space constraints involved in utilizing a wind generation device while also presenting the versatility of allowing the wind field to be defined numerically and testing different turbines without the need to design a specific scale model for each setup. This work considered a winch system actuator emulating only the thrust forces. The results showed that the winch will lag at higher frequencies, which for the conditions tested, was not very relevant considering the sea spectrum utilized, and also the line pre-tension might cause a slight shift on the system's pitch and surge eigenfrequencies. By replicating just the thrust force, part of the dynamics is also hindered, using more cables pulling from different directions would be ideal but it still has to be taken into account that the extra force emulation will come at the expense of more space usage and increased complexity.

Similarly to the wind tunnel HiL, the aerodynamic model also needs simplifications to run in real-time, utilizing fully rigid blades, a simple BEM model is used and the number of blade elements is minimized. Concerning the results, the hybrid setup presented more variations, with the statistics diverging from FAST and MSWT at 13 m/s and presenting a more comparable response to the lower thrust case, 21 m/s. The main differences were observed especially at the pitch natural frequency, where the aerodynamic damping remained similar for both cases with the MSWT and numerical simulation yet with contradictory results for the winch. At wave frequency, the experimental setups and numerical simulations presented a very similar behavior.

In conclusion, each experimental setup presented its nuances. Disparities were observed when comparing to numerical models and potential reasons for the observable differences were listed. As a recommendation for future works, more cross-comparison is needed between the experimental approaches, preferably done simultaneously or iteratively in order to dimmish uncertainties and promote more exchange of information between the testing facilities. At last, the experimental data presented here were from two test campaigns performed in the past that were not initially thought to be used as a direct comparison. Future joint experimental campaigns could focus on replicating also the same conditions at both facilities.

7. Bibliography

Bak, C., Zahle, F., Bitsche, R., Kim, T., Yde, A., Henriksen, L. C., Nata-rajan, A., and Hansen, M. H.: Department of Wind Energy I-Report Description of the DTU 10 MW Reference Wind Turbine, 2013.

Bayati, I., Belloli, M., Bernini, L., and Zasso, A.: Wind tunnel validation of AeroDyn within LIFES50+ project: imposed Surge and Pitch tests, Journal of Physics: Conference Series, 753, 092001, https://doi.org/10.1088/1742-6596/753/9/092001, 2016c.

Bayati, I., Belloli, M., Bernini, L., Mikkelsen, R., and Zasso, A.: On the aero-elastic design of the DTU 10MW wind turbine blade for the LIFES50+ wind tunnel scale model, Journal of Physics: Conference Series, 753, 022028, https://doi.org/10.1088/1742 6596/753/2/022028, 2016.

Bayati, I., Facchinetti, A., Fontanella, A., and Belloli, M.: 6-DoF Hydrodynamic Modelling for Wind Tunnel Hybrid/HIL Tests of FOWT: The Real-Time Challenge, Volume 10: Ocean Renewable Energy, V010T09A078, https://doi.org/10.1115/OMAE2018-77804, 2018.

Bergua, R., Robertson, A., Jonkman, J., Branlard, E., Fontanella, A., Belloli, M., Schito, P., Zasso, A., Persico, G., Sanvito, A., Amet, E., Brun, C., Campaña Alonso, G., Martín-San-Román, R., Cai, R., Cai, J., Qian, Q., Maoshi, W., Beardsell, A., Pirrung, G., Ramos-García, N., Shi, W., Fu, J., Corniglion, R., Lovera, A., Galván, J., Nygaard, T. A., dos Santos, C. R., Gilbert, P., Joulin, P.-A., Blondel, F., Frickel, E., Chen, P., Hu, Z., Boisard, R., Yilmazlar, K., Croce, A., Harnois, V., Zhang, L., Li, Y., Aristondo, A., Mendikoa Alonso, I., Mancini, S., Boorsma, K., Savenije, F., Marten, D., Soto-Valle, R., Schulz, C. W., Netzband, S., Bianchini, A., Papi, F., Cioni, S., Trubat, P., Alarcon, D., Molins, C., Cormier, M., Brüker, K., Lutz, T., Xiao, Q., Deng, Z., Haudin, F., and Goveas, A.: OC6 project Phase III: validation of the aerodynamic loading on a wind turbine rotor undergoing large motion caused by a floating support structure, Wind Energy Science, 8, 465–485, https://doi.org/10.5194/wes-8-465-2023, 2023.

DNV-GL- RP-0286. Coupled analysis of floating wind turbines. 2019.

DNV-GL. The power to commercialize. 2020.

E. E. Bachynski, V. Chabaud, and T. Sauder. Real-time hybrid model testing of floating wind turbines: Sensitivity to limited actuation.EnergyProcedia, 80:2–12, 2015. 12th Deep Sea Offshore Wind RD Conference,EERA DeepWind'2015.

Fontanella, A., Bayati, I., Mikkelsen, R., Belloli, M., and Zasso, A.: UNAFLOW: a holistic wind tunnel experiment about the aerodynamic response of floating wind turbines under imposed surge motion, Wind Energy Science, 6, 1169–1190, https://doi.org/10.5194/wes-6-1169-2021, 2021.

Fowler, M. J., Kimball, R. W., Thomas III, D. A., and Goupee, A. J.: Design and testing of scale model wind turbines for use in wind/wave basin model tests of floating offshore wind turbines, 55423, V008T09A004, 2013.

Gaertner, E., Rinker, J., Sethuraman, L., Zahle, F., Anderson, B., Barter, G., Abbas, N., Meng, F., Bortolotti, P., Skrzypinski, W., Scott, G., Feil, R., Bredmose, H., Dykes, K., Sheilds, M., Allen, C., and Viselli, A.: Definition of the IEA 15-Megawatt Offshore Reference Wind.

Goupee, A. J., Koo, B. J., Kimball, R. W., Lambrakos, K. F., and Dagher, H. J.: Experimental Comparison of Three Floating Wind Turbine Concepts, Journal of Offshore Mechanics and Arctic Engineering, 136, 020 906, https://doi.org/10.1115/1.4025804, 2014.

Goupee, A. J., Koo, B., Lambrakos, K., and Kimball, R.: Model Tests for Three Floating Wind Turbine Concepts, All Days, OTC–23470 MS, https://doi.org/10.4043/23470-MS, 2012.

Gueydon, S., 2016. Aerodynamic damping on a semisubmersible floating foundation for wind turbines. Energy Procedia 94, 367–378. https://doi.org/10.1016/j. egypro.2016.09.196.

GWEC: Report: Floating Offshore Wind - A Global Opportunity, 2022.

I. Bayati, A. Facchinetti, A. Fontanella, F. Taruffi, and M. Belloli. Analysis of FOWT dynamics in 2-DOF hybrid HIL wind tunnel experiments. Ocean Engineering, 195:106717, 2020.

Jonkman, B. and Jonkman, J.: FAST v8.16.00a-bjj, 2016.

Jonkman, J., Butterfield, S., Musial, W., and Scott, G.: Definition of a 5-MW Reference Wind Turbine for Offshore System Development, 2009, https://doi.org/10.2172/947422.

LIFES50+. D7.9 Guidance and Recommended Methods for Hybrid/HIL-based FOWT Experimental Testing. 2015.

M. Belloli, I. Bayati, A. Facchinetti, A. Fontanella, H. Giberti, F. La Mura,F. Taruffi, and A. Zasso. A hybrid methodology for wind tunnel testing of floating offshore wind turbines.Ocean Engineering, 210:107592, 2020.

M. Hall, J. Moreno, and K. Thiagarajan. Performance Specifications for Real-Time Hybrid Testing of 1:50-Scale Floating Wind Turbine Models. Volume 9B: Ocean Renewable Energy, 06 2014.

M. Thys, A. Fontanella, F. Taruffi, M. Belloli, and P. A. Berthelsen. Hybrid Model Tests for Floating Offshore Wind Turbines. ASME 2019 2ndInternational Offshore Wind Technical Conference, 11 2019.

Martin, H. R., Kimball, R. W., Viselli, A. M., and Goupee, A. J.: Methodology for wind/wave basin testing of floating offshore wind turbines, Journal of Offshore Mechanics and Arctic Engineering, 136, 020 905, 2014.

Müller, K., Sandner, F., Bredmose, H., Azcona, J., Manjock, A., and Pereira, R.: Improved tank test procedures for scaled floating offshore wind turbines, 2014.

Otter, A., Murphy, J., Pakrashi, V., Robertson, A., and Desmond, C.: A review of modelling techniques for floating offshore wind turbines,170 Wind Energy, 25, 831–857, https://doi.org/https://doi.org/10.1002/we.2701, 2022.

Robertson, A. N., Wendt, F., Jonkman, J. M., Popko, W., Dagher, H., Gueydon, S., Qvist, J., Vittori, F., Azcona, J., Uzunoglu, E., Soares, C. G., Harries, R., Yde, A., Galinos, C., Hermans, K., de Vaal, J. B., Bozonnet, P., Bouy, L., Bayati, I., Bergua, R., Galvan, J., Mendikoa, I., Sanchez, C. B., Shin, H., Oh, S., Molins, C., and Debruyne, Y.: OC5 Project Phase II: Validation of Global Loads of the DeepCwind Floating Semisubmersible Wind Turbine, Energy Procedia, 137, 38–57, https://doi.org/https://doi.org/10.1016/j.egypro.2017.10.333, 14th Deep Sea Offshore Wind RD Conference, EERA DeepWind'2017, 2017.

S. Gueydon, I. Bayati, and E. de Ridder. Discussion of solutions for basin model tests of FOWTs in combined waves and wind. Ocean Engineering,209:107288, 2020.

S. Gueydon, R. Lindeboom, W. van Kampen, and E.-J. de Ridder. Comparison of Two Wind Turbine Loading Emulation Techniques Based on Tests of a TLP-FOWT in Combined Wind, Waves and Current. ASME 2018 1stInternational Offshore Wind Technical Conference, 11 2018.

Taruffi, F., Novais, F., and Viré, A.: An experimental study on the aerodynamic loads of a floating offshore wind turbine under imposed motions, Wind Energy Science, 9, 343–358, https://doi.org/10.5194/wes-9-343-2024, 2024.

van Kuik, G. A. M., Peinke, J., Nijssen, R., Lekou, D., Mann, J., Sørensen, J. N., Ferreira, C., van Wingerden, J. W., Schlipf, D., Gebraad, P., Polinder, H., Abrahamsen, A., van Bussel, G. J. W., Sørensen, J. D., Tavner, P., Bot155 tasso, C. L., Muskulus, M., Matha, D., Lindeboom, H. J., Degraer, S., Kramer, O., Lehnhoff, S., Sonnenschein, M., Sørensen, P. E., Künneke, R. W., Morthorst, P. E., and Skytte, K.: Long-term research challenges in wind energy – a research agenda by the European Academy of Wind Energy, Wind Energy Science, 1, 1–39, https://doi.org/10.5194/wes-1-1-2016, 2016.

Wendt, F. F., Robertson, A. N., and Jonkman, J. M.: FAST Model Calibration and Validation of the OC5-DeepCwind Float-ing Offshore Wind System Against Wave Tank Test Data, International Journal of Offshore and Polar Engineering, 29, 15–23,https://doi.org/10.17736/ijope.2019.jc729, 2019.